UTD-Based Modeling of Diffraction Loss by Dielectric Circular Cylinders at D-band

Seunghwan Kim
School of Electrical and Computer Engineering
Georgia Institute of Technology
Atlanta, GA 30332 USA

Abstract— **This paper presents modeling of diffraction loss caused by dielectric circular cylinders obstructing the LOS path at the center frequency of D-band (140 GHz). UTD approach to the problem in order to predict the diffraction loss introduced by a coffee mug on a desktop is investigated. The results are compared with D-band measurements with very good agreement between them, which confirms the existence of rays that diffract off the convex surfaces of the cylinder. The finding can be extended to OLoS scenarios for indoor environment with moving persons as studies have shown that human torso can be modelled with a cylinder filled with salt water. The results can contribute to the accurate modeling of future high-data-rate D-band indoor channels by predicting the loss caused by signals obstructed by human bodies.**

I. INTRODUCTION

For short-range device-to-device desktop communication channels, it is rarely the case that Line-of-Sight (LoS) path is always available. Since LoS is very likely to be obstructed by objects of variety of shapes and materials, channel models have to take into account NLoS communication. Obstruction of LoS is especially more problematic for high-frequency indoor applications due to the high free-space path loss. Therefore, for NLoS scenarios at high frequencies, it is critical to understand which propagation mechanism (i.e., reflection, diffraction, or scattering) prevails, and how much loss is associated with it, such that path loss can be correctly predicted and the viability of the NLoS link is verified. While D-band (110~170 GHz) has been proposed as a promising band for future ultra-fast, ultra-wideband wireless communications [1], not much research has been reported on how these high frequency signals behave when perturbed by objects of various shapes and materials in both indoor and outdoor scenarios. In desktop environment, which offers a suitable range for D-band communications, objects of cylindrical shape (e.g., cups and bottles) can serve as common obstruction of LoS paths between devices. Here, the presence of "creeping waves", or surface-diffracted rays, is of great interest in maintaining the communication link, and to verify it, in this paper, Uniform Geometrical Theory of Diffraction (UTD) will be employed to model the diffraction loss at the receiver location. Finally, the result will be compared with the measurement for validation.

The remainder of this paper is organized as follows: Section II briefly describes the measurement campaign. In Section III, diffraction loss by the cylindrical obstruction is modeled at 140 GHz and compared with the measurement, and finally, concluding remarks and future work are presented in Section V.

II. MEASUREMENT SCENARIO

The complex S21 is measured with the D-band transmission system and a vector network analyzer in the OLoS environment, where the ceramic mug, initially located at the center of LoS, is gradually moved away from the LoS along a trajectory perpendicular to the LoS in 2 mm increment. The separation distance between the Tx and Rx test heads is 86.46 cm. The diffraction loss is measured as the difference in the S21 between the LoS case and when the obstruction is present. Details of the equipment and measurement parameters are omitted here due to spatial limitation, but can be found in [1].

III. DIFFARACTION LOSS MODELING

Fig. 1 shows the mathematical representation of the diffraction loss measurement scenario described in Section II. The movement of the cylindrical obstruction along a trajectory perpendicular to LoS has been translated as the moving source and observation points, P and S, while the cylinder's center is fixed at the origin. As shown in Fig. 1, the displacement of P and S is denoted as *c,* and it follows that, when $c < b$, the observation point, S, is in the Shadow Region, while, for $c \geq b$, S is in the Lit Region. In the Shadow Region, according to UTD, there are two surface-diffracted rays, travelling clock-wise and counter-clock-wise around the cylinder [2] as shown in Fig. 2. Hence, the total E-field at the observation point, S_o, is determined by the sum of these two rays. The E-fields associated with each ray at S_0 can be mathematically expressed as [2]

$$E_1{}^d(S_0) = E^i(Q'_1) \cdot T_{s,h1} \cdot \frac{e^{-jks_1{}^d}}{\sqrt{s_1{}^d}} \quad (1)$$

$$E_2{}^d(S_0) = E^i(Q'_2) \cdot T_{s,h2} \cdot \frac{e^{-jks_2{}^d}}{\sqrt{s_2{}^d}}, \quad (2)$$

Fig. 1. 2-D translation of the diffraction loss measurement onto the Cartesian plane.

where $T_{s,h}$ is the UTD diffraction coefficient; $E_i(Q_1')$ and $E_i(Q_2')$ are the E-fields incident at Q_1' and Q_2', respectively, which are expressed as

$$E^i(Q'_1) = \frac{e^{-jks_1'}}{\sqrt{s_1'}} \quad (3)$$

$$E^i(Q'_2) = \frac{e^{-jks_2'}}{\sqrt{s_2'}}. \quad (4)$$

In the Lit Region, on the other hand, the total field at the observation point, S_n, is determined by the contributions from the direct LoS ray and the reflected ray as shown in Fig. 3, and the fields associated with each ray can be written as [2]

$$E^i(S_n) = \frac{e^{-jks^{LOS}}}{\sqrt{s^{LOS}}} \quad (5)$$

$$E^r(S_n) = E^i(Q_r) \cdot R_{s,h} \cdot \sqrt{\frac{\rho^r}{\rho^r + s^r}} \cdot e^{-jks^r}, \quad (6)$$

where $R_{s,h}$ is the UTD reflection coefficient, and $E_i(Q_r)$, the incident field at the reflection point, Q_r, is expressed as

$$E^i(Q_r) = \frac{e^{-jks^i}}{\sqrt{s^i}}. \quad (7)$$

Calculations of $T_{s,h}$ and $R_{s,h}$ are omitted here, but can be found in [2]. In (6), ρ_r represents the caustic distance of the reflected ray tube, which can be calculated as following [2]:

$$\frac{1}{\rho^r} = \frac{1}{\rho^i(Q_r)} + \frac{2}{a_0(Q_r)cos\theta^i}, \quad (8)$$

where $\rho_i(Q_r)$ is equivalent to s^i, and $a_0(Q_r)$ denotes the radius of curvature at the reflection point, Q_r. All parameters in (1) ~ (8) are shown in Fig. 2 and 8. It is also observed from Fig. 3 that there exists a third ray reaching the observation point, which is equivalent to surface-diffracted ray 2 from Fig. 2.

The total E_z fields in the Shadow and Lit Regions can finally be expressed as a sum of the field components defined in (1), (2), (5), and (6):

$$E_z^{tot} = \begin{cases} E_z^{d1} + E_z^{d2}, & 0 < c < b \quad - \quad Shadow\ Region \\ E_z^i + E_z^r + E_z^{d2}, & c \geq b \quad - \quad Lit\ Region \end{cases} \quad (9)$$

Fig. 4 shows how the four field components, namely, the two surface-diffracted fields, direct incident field, and the reflected field, vary their magnitudes as the cylinder obstruction is moved away from LoS, or as c from Fig. 1 varies from 0 to 10 cm. Since the mug's outer radius, or b, has been set to 5 cm, the shadow boundary is located at $c = b = 5$ cm; c values less than that means that observation point is in the Shadow Region, while c greater than 5 cm corresponds to the Lit Region. In Fig. 4, it is observed that, initially, when the mug is totally blocking the LoS, the two surface-diffracted fields have

Fig. 2. Field components in the Shadow Region

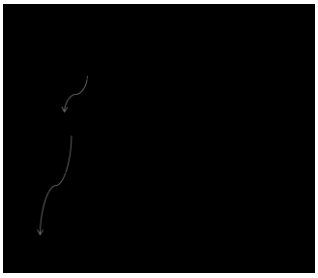

Fig. 3. Field components in the Lit Region

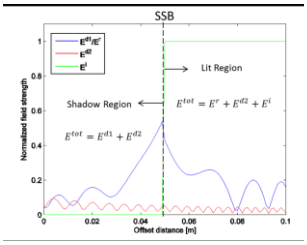

Fig. 4. Variations in E-field components with respect to the mug offset distance, c

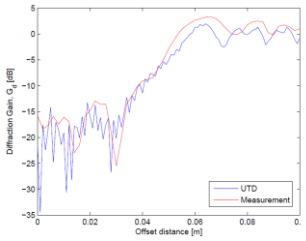

Fig. 5. Comparison between UTD modeled and measured diffractions losses at f=140 GHz

the same magnitudes, but as c, the offset distance, increases, the second diffracted field, E^{d2}, keeps decreasing, while E^{d1} increases. This is due to the fact that the total distance the first surface-diffracted ray travels decreases, while the second surface-diffracted ray travels increasingly longer distance as the mug offset increases. It is also observed from Fig. 4 that when c reaches b, or the shadow boundary, the observation point now enters the Lit Region, and the first surface-diffracted ray is translated to the reflected ray that starts decreasing with increasing c. Meanwhile, in this lit region, the direct LoS incident field, E_i, is now present, while the second surface-diffracted field still exists with small amplitude. Finally, the diffraction losses calculated with the square magnitudes of the total E_z fields are plotted with respect to the mug offset distance, and compared with the measured diffraction loss in Fig. 5. As can be observed, the UTD modeled diffraction loss for the dielectric cylinder obstruction at D-band very closely predicts the measurement. The oscillation at 0 dB level is due to the constructive and destructive interference among the three rays present in the Lit Region, namely, the incident, reflected, and surface-diffracted rays as illustrated in Fig. 3.

IV. Conclusion

This paper presented modeling of diffraction loss caused by a dielectric cylinder obstruction at 140 GHz using UTD. Comparison with the measurement revealed that the diffraction loss can be accurately estimated with UTD, which confirms the existence of surface-diffracted rays. The finding can be extended to OLoS scenarios for indoor environment with moving persons, which is the next step in this research, as studies have shown that human torso can be modelled with a cylinder filled with salt water [3]. The results can contribute to the accurate modeling of future high-data-rate D-band indoor channels by predicting the loss caused by signals obstructed by human bodies.

References

[1] S. Kim, W.T. Khan, A. Zajic, and J. Papapolymerou, \D-Band Channel Measurements and Characterization for Indoor Applications," IEEE Transactions on Antennas and Propagation, vol. 63, pp. 3198-3207, July 2015.

[2] D. A. McNamara, et al, "Introduction to the Uniform Geometrical Theory of Diffraction", Artech House, MA, 1990.

[3] R. Saadane, A. Khafaji, J. El Abbadi, and M. Belkasmi, "The influence of people shadowing on the modelling of 60 GHz Band propgation," *Recent Advances in Technoolgoies*, Intech, pp. 275–290, Nov. 2009.